A Winter Short Course on Statistical Mechanics for Molecular Simulations

Lecture 6: Applications of Dissipative Particle Dynamics and Dynamical Monte Carlo Method

Yuan-Chung Cheng
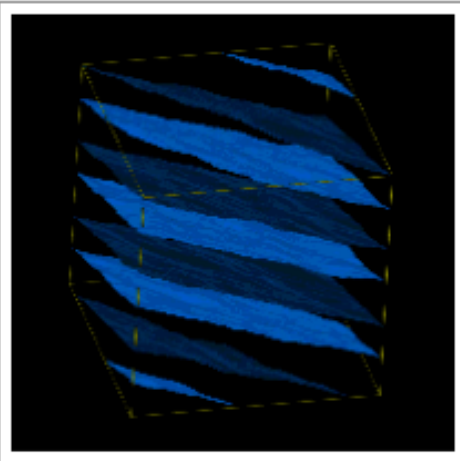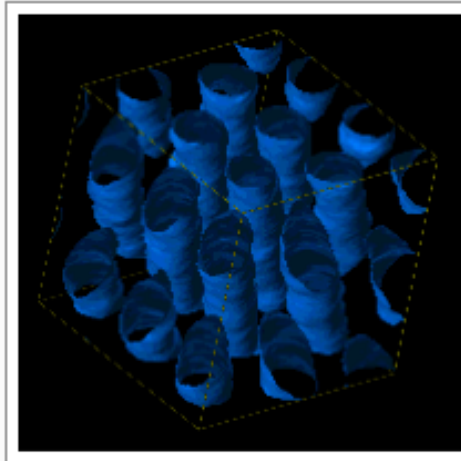yuanchung@ntu.edu.tw
2/11/2015

DPD Examples

- ## DPD references:
  - ☐ Dissipative particle dynamics: Bridging the gap between atomistic and mesoscopic simulation by Groot and Warren in J. Chem. Phys., 107, 4423 (1997).

  - ☐ Statistical Mechanics of Dissipative Particle Dynamics by Espanol & Warren in Europhys. Lett., 30, 191 (1995).
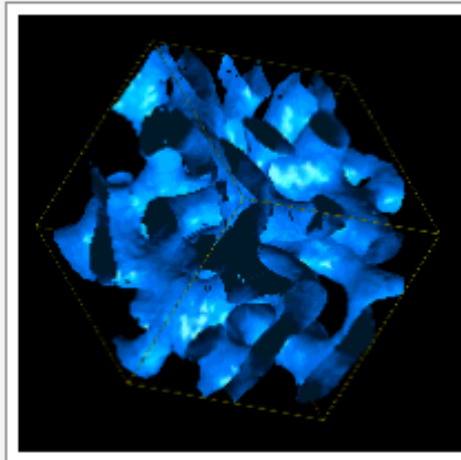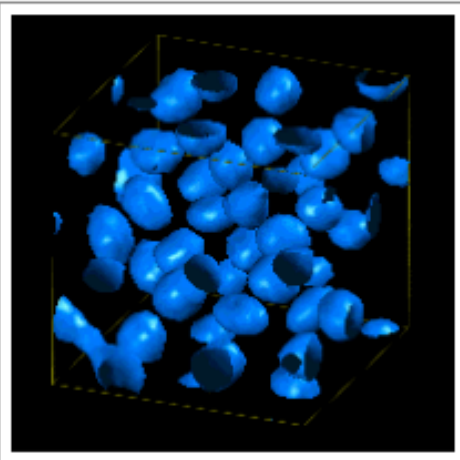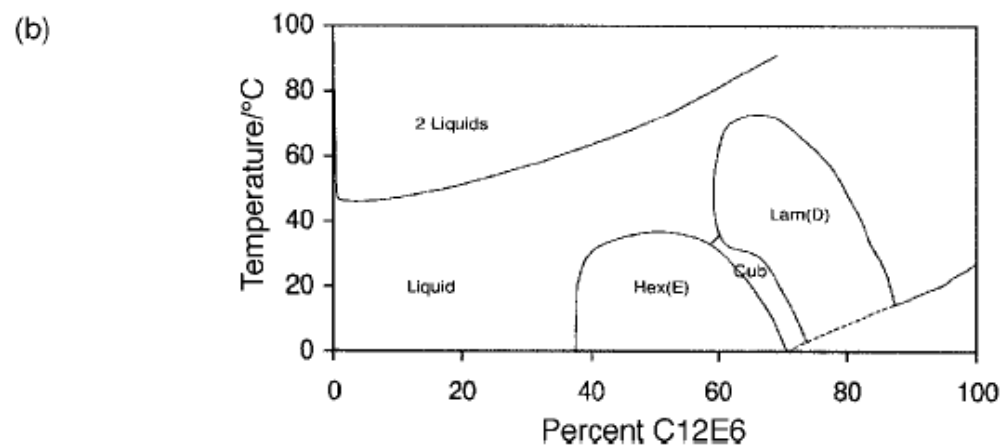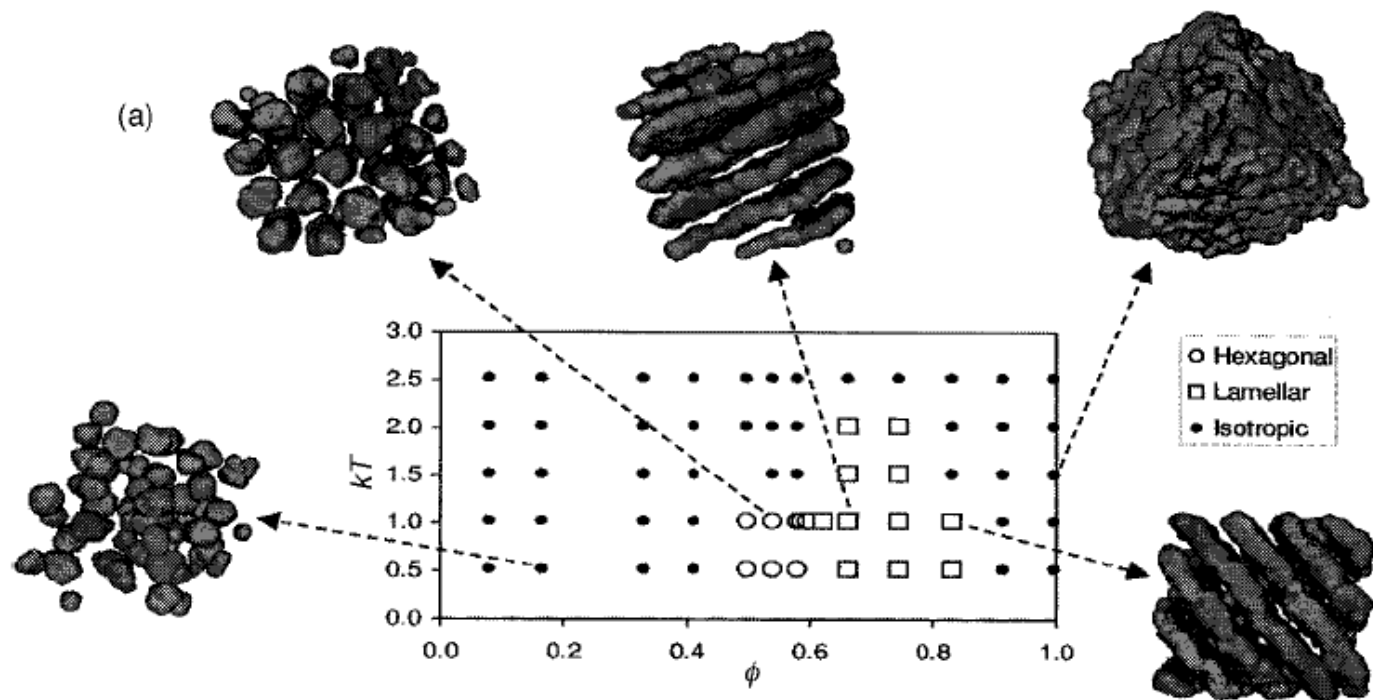
A5B5

A3B7

A2B8

Correct hydrodynamics require for rapid phase formation

Morphology of copolymer blends with varying ratios of head-to-tail group size.

R. D. Groot and T. J. Madden, *J. Chem. Phys.* **108**, 8713 (1998).

Fig. 1 (a) Top: Phase diagram for DPD dimers. Energy parameters and composition variables are defined in the text. (b) Bottom: Experimental phase diagram for a nonionic surfactant, from ref. 16. Colour representations of these figures are available as supplementary material. Details are available from the Editorial office. For electronic access see http://www.rsc.org/suppdata/cp/1999/2051.

- Movie for Simulation of A3B7 block copolymer melt (a3b7-sm.mpg)

(http://www.apmaths.uwo.ca/~mkarttu/dpd.shtml)

Mesoscopic simulation of self-assembly using dissipative particle dynamics

Researchers: Mikko Karttunen, Ilpo Vattulainen[*],Gerhard Besold[#] , James Polson[+], Petri Nikunen
# Max Planck Institute for Polymer Research, Mainz, Germany
[*]Technical Univ. of Denmark/Helsinki University of Technology
[+]University of Prince Edward Island, Charlottetown, Canada

Project home page

Dissipative Particle Dynamics (DPD) is a mesoscopic simulation technique which is particularly well suited for studies of soft condensed matter systems. It is characterized by coarse-graining in particle representation leading to a simplified description of interparticle interactions in terms of conservative, dissipative, and random forces. This formulation leads to momentum conservation, which implies that *hydrodynamic flow effects* are properly taken into account.

We use DPD to study the self-assembly of lipid bilayers and the formation of complex structures in polymer and lipid systems, see Figs. 27a and b. Self-assembly is cooperative process, and its many-particle nature together with the presence of many time and length scales poses many interesting challenges. Our main interest lies in lipid and polymeric systems containing charges. Practical applications include, for example, drug delivery by cationic liposomes, detergents and emulsions.
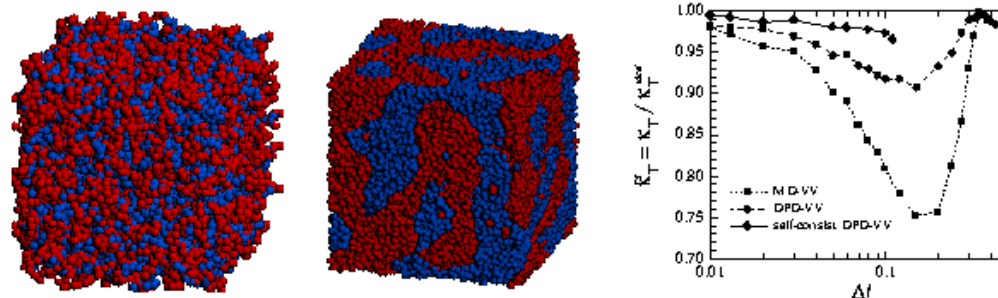

Figure 27: *DPD simulation of symmetric 5-5 block co-polymer melt consisting of 40000 monomers. a) The initial state is completely disordered. b) During the simulation the system undergoes microphase separation. The snapshot is after 2000 time steps. c) It is important to choose a proper way to integrate the equations of motion. This is illustrated by plotting the ideal gas compressibility as a function of the time step for three different integration methods. Any deviations from one indicate artifacts.*

The DPD method poses some practical problems, and during the first stage of this project we have studied the quality of various DPD integrators in terms of physical observables, such as response functions and transport coefficients. Due to the presence of stochastic and velocity-dependent dissipative forces, integration of the equations of motion may give rise to pronounced artifacts, see Fig. 27c. We have shown that artifacts can be sufficiently suppressed by using integrator schemes in which the velocity dependence of the dissipative forces is taken into account.
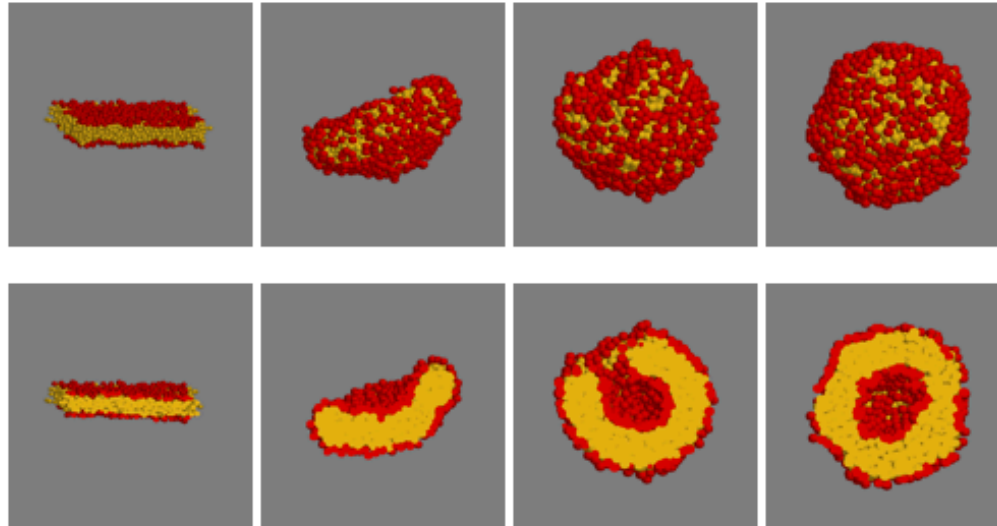
Liposome Formation

Liposome (微脂體)
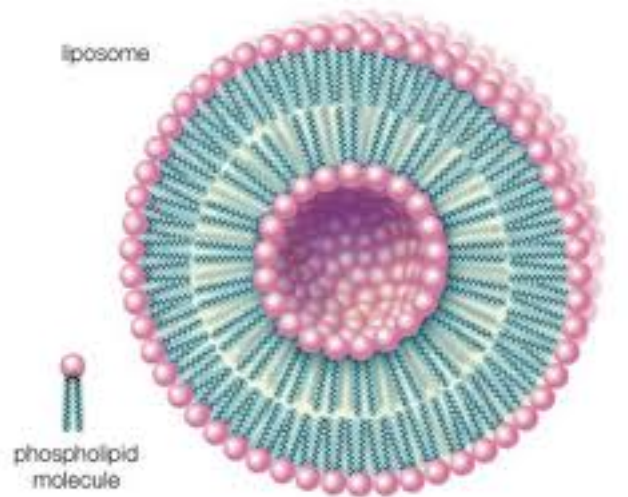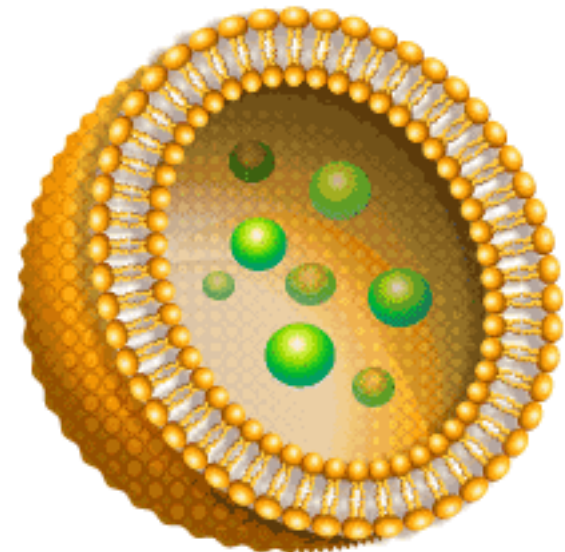
Liposome

Also good for drug delivery, protein encapsulation…

Liposome Formation

DPD Simulation of liposome formation:

- Below are snapshots of a DPD simulation of liposome formation (Nikunen, Karttunen & Vattulainen). The second row shows a cross-section of the system. Water has been removed for clarity.

- The system has roughly 86000 particles.

Dynamics important for content encapsulation processes

http://www.apmaths.uwo.ca/~mkarttu/dpd.shtml

- Movie for liposome formation dynamics:

  large version: lipo1.mpg
  small, space filled: formation.mpg
  small, cross section: formation3.mpg

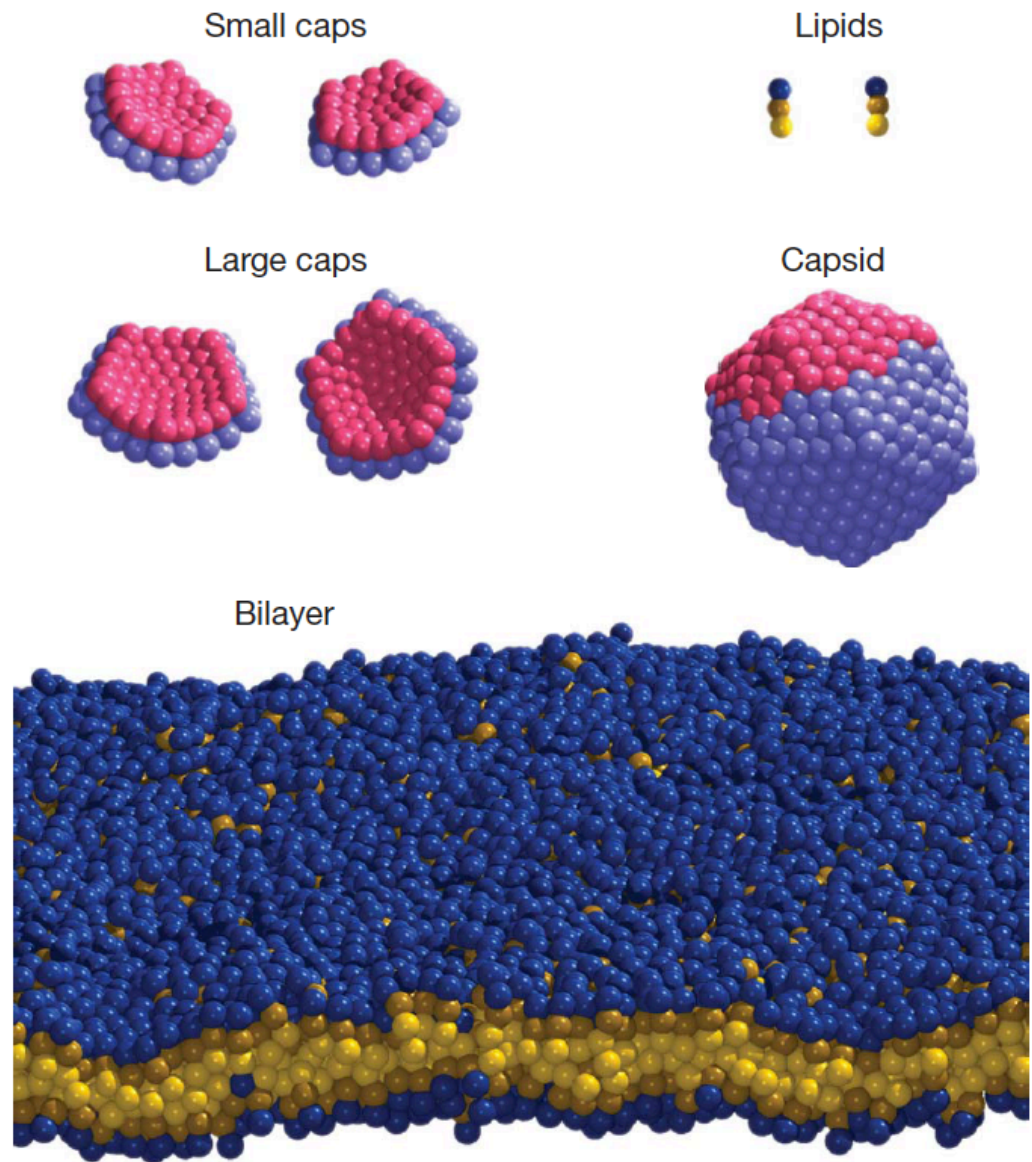 (http://www.apmaths.uwo.ca/~mkarttu/dpd.shtml)

LETTERS

Aggregation and vesiculation of membrane proteins by curvature-mediated interactions

Benedict J. Reynwar[1], Gregoria Illya[1], Vagelis A. Harmandaris[1], Martin M. Müller[1], Kurt Kremer[1] & Markus Deserno[1]

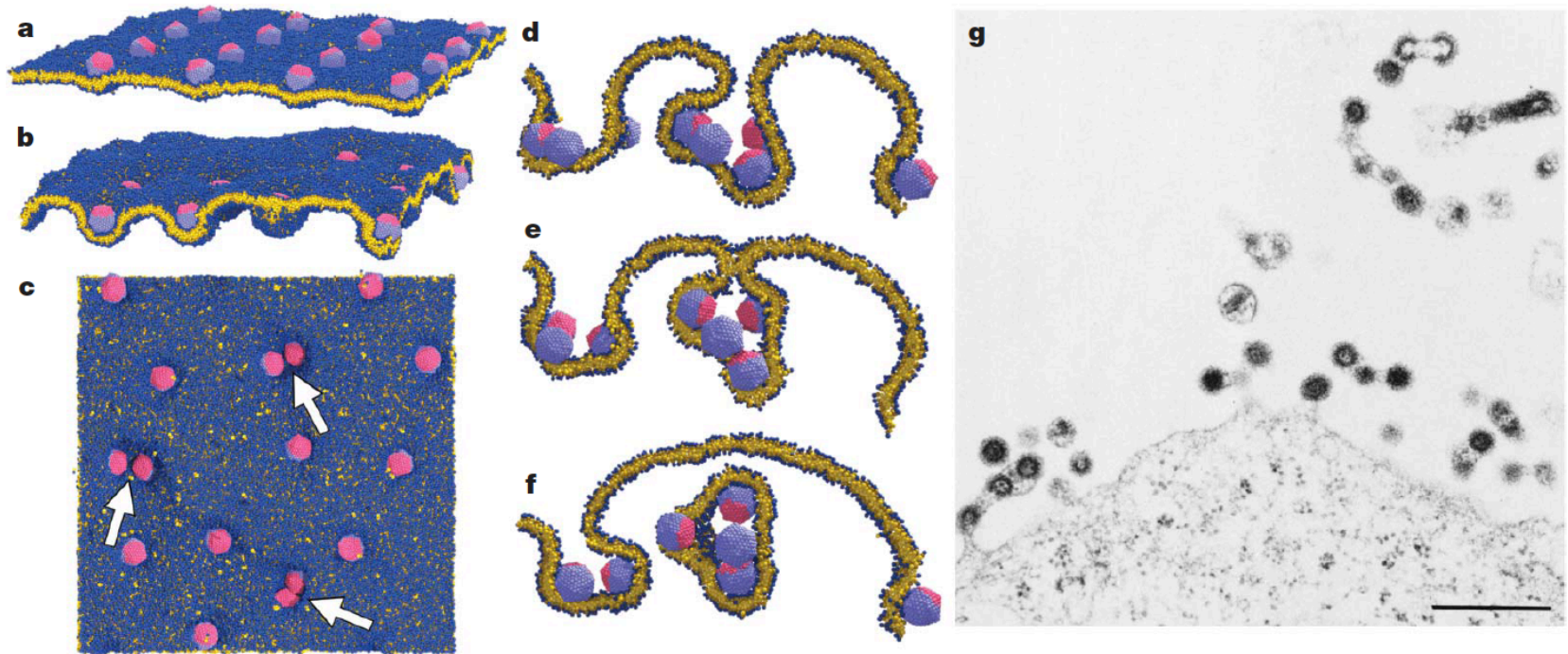Small caps

Lipids

Large caps

Capsid

Bilayer

Figure 1 | Illustration of the individual entities used in the simulation.
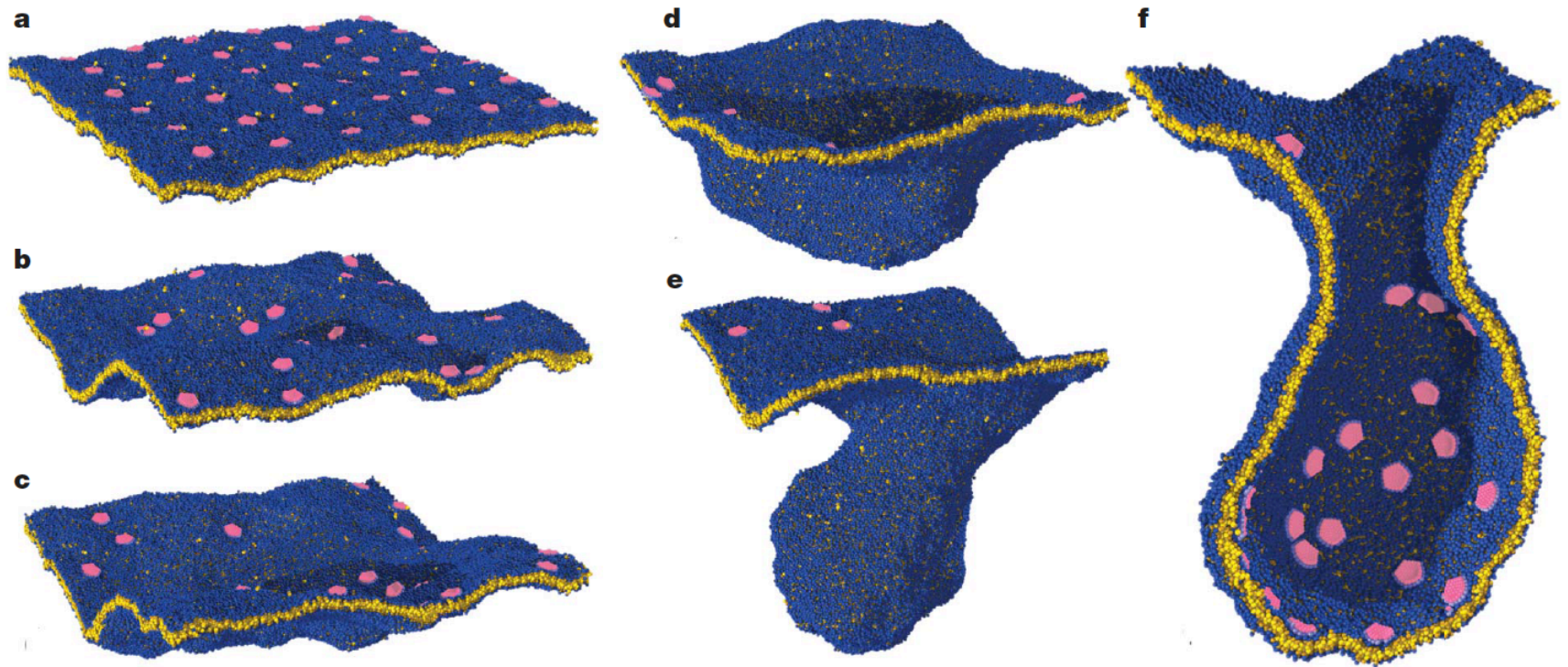
Figure 2 | Successive stages of a vesiculation event driven by 36 large caps on a membrane containing 46,080 lipids. The times of the simulation snapshots are: **a**, 0τ; **b**, $20,000\tau$; **c**, $40,000\tau$; **d**, $50,000\tau$; **e**, $60,000\tau$; and **f**, $70,000\tau$, the last corresponding to roughly 1 ms.

Figure 3 | Attraction and cooperative budding driven by 16 capsids on a membrane containing 40,960 lipids. a–f, A series of simulation snapshots. The times are: **a**, 0τ; **b**, $1{,}000\tau$; **c**, $7{,}000\tau$; **d**, $16{,}000\tau$; **e**, $17{,}000\tau$; and **f**, $18{,}000\tau$, the last corresponding to roughly 0.3 ms. The arrows in **c** point to formed capsid-pairs. The slices **d**–**f** indicate cooperative budding, a phenomenon also seen in the electron micrograph (**g**) of late domain–mutated MPMV virions (scale bar, 500 nm; reprinted from ref. 28 with permission of authors and publisher; copyright 2003, The American Society for Microbiology).
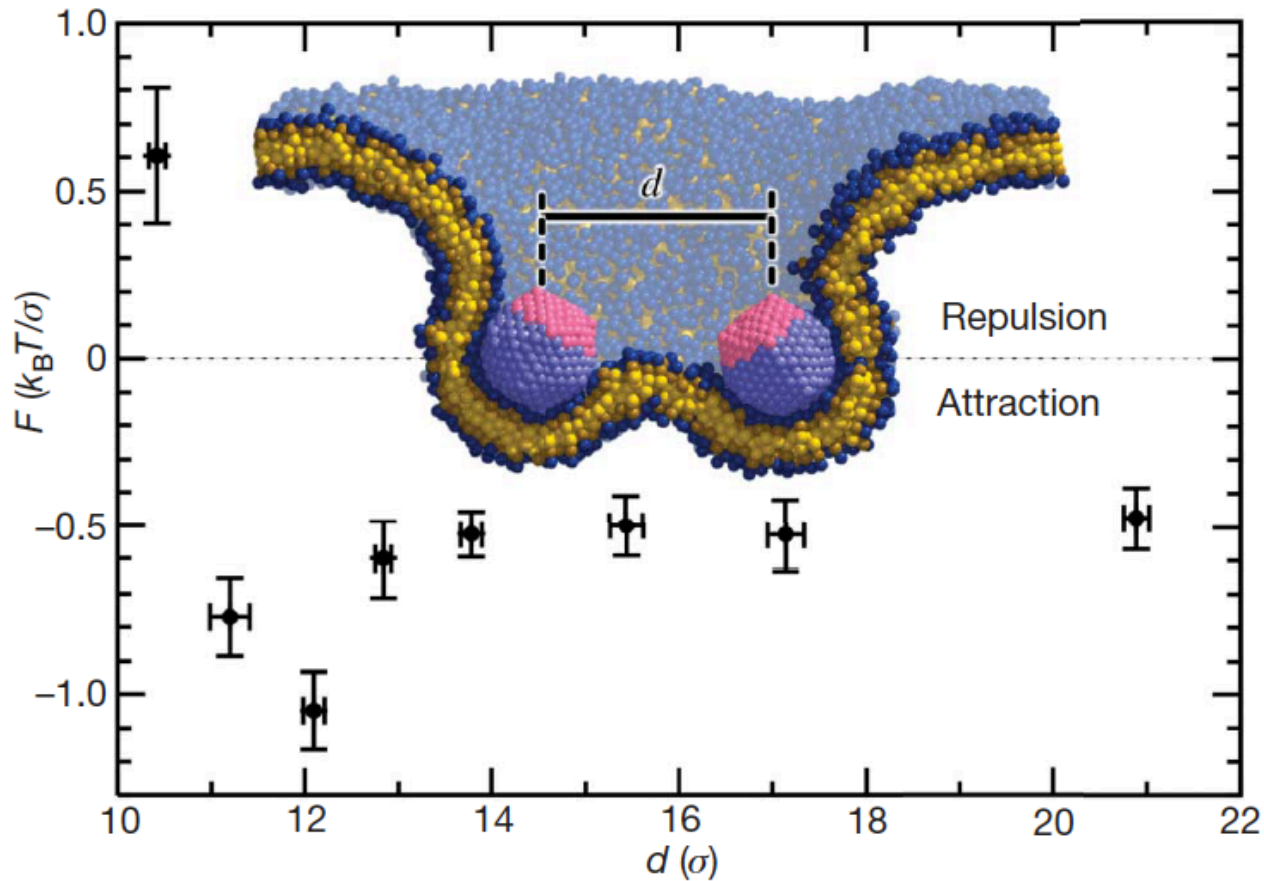
Figure 4 | Force versus distance for two capsids. Negative forces signify attraction. Vertical error bars, ±1 s.e.m.; horizontal error bars, ±1 s.d. Inset, a cross-sectional cut through the membrane profile for a separation of $d = 21\sigma$.

Membrane curvature induced collective behavior

Dynamic capillary wetting studied with dissipative particle dynamics

Claudio Cupelli[1,4], Björn Henrich[2,3], Thomas Glatzel[1], Roland Zengerle[1], Michael Moseler[2,3] and Mark Santer[1,3]

[1] Laboratory for MEMS applications, Department of Microsystems Engineering (IMTEK), University of Freiburg, Georges-Koehler-Allee 106, 79110 Freiburg, Germany
[2] Freiburg Materials Research Center (FMF), Stefan-Meier-Straße 21, 79104 Freiburg, Germany
[3] Fraunhofer Institute for Mechanics of Materials IWM, Wöhlerstraße 11, 79108 Freiburg, Germany
E-mail: cupelli@imtek.de
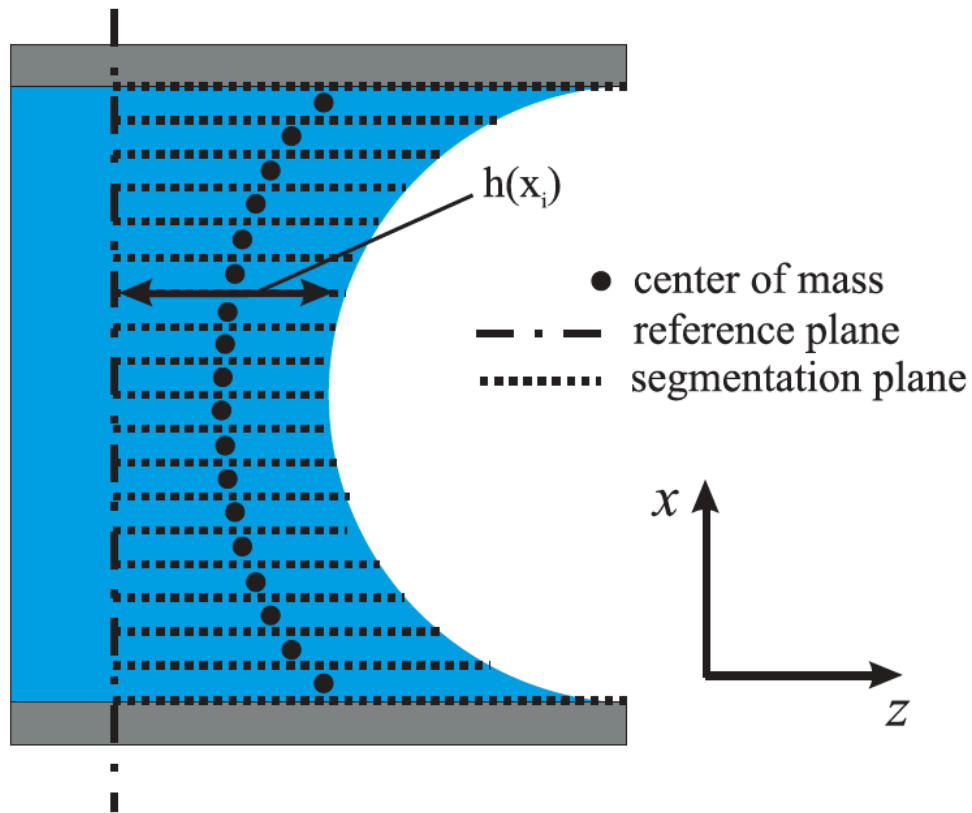
**Figure 2.** Scheme of the set-up used for determining the static contact angle. The center of mass in each slab is determined separately and averaged over 1000 time steps in order to determine the shape of the meniscus.
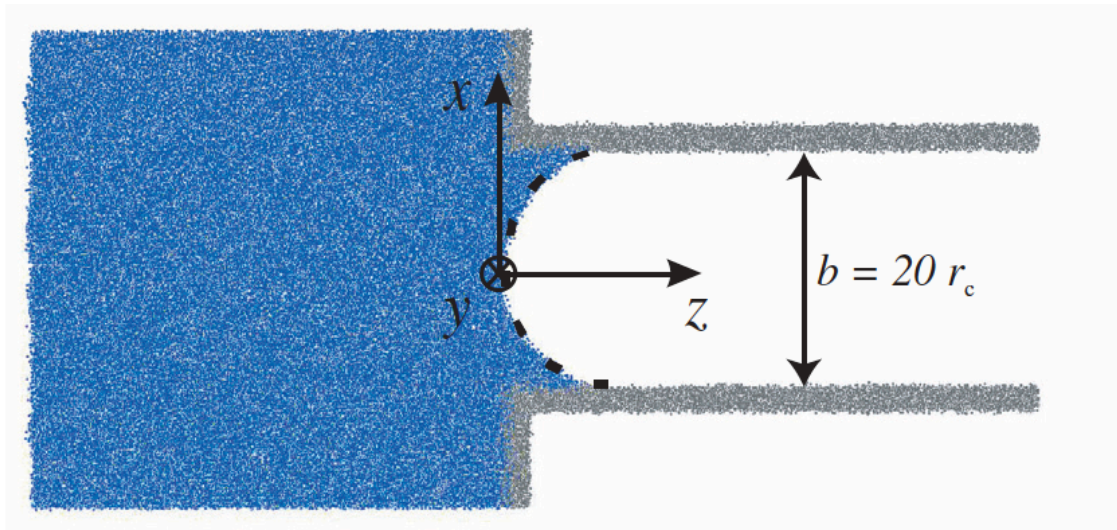
Figure 7. Set-up for capillary impregnation. The meniscus penetrates in the z-direction due to the driving capillary pressure. Periodic boundary conditions are applied in the y-direction and in the x-direction. The shape of the meniscus and the penetration depth is monitored by segmenting the pore into 20 slabs and evaluating the center of mass in each slab separately as in figure 2.
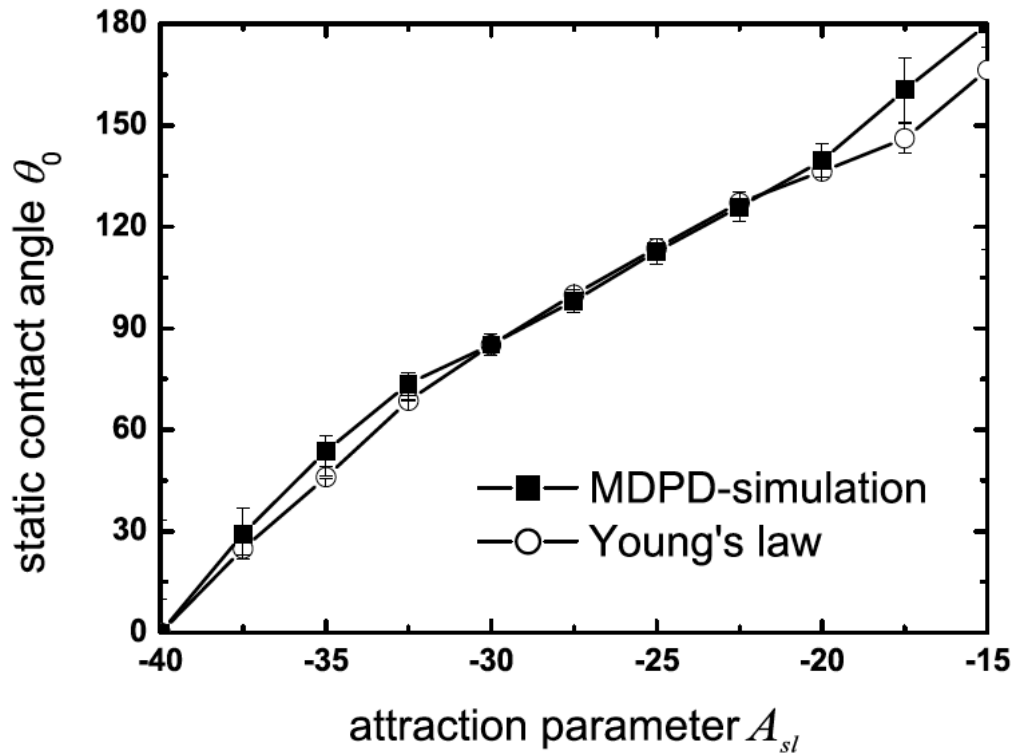
Figure 3. Comparison of Young's law (circles) and the result of the MDPD-simulation (squares). Vertical axis in degrees.
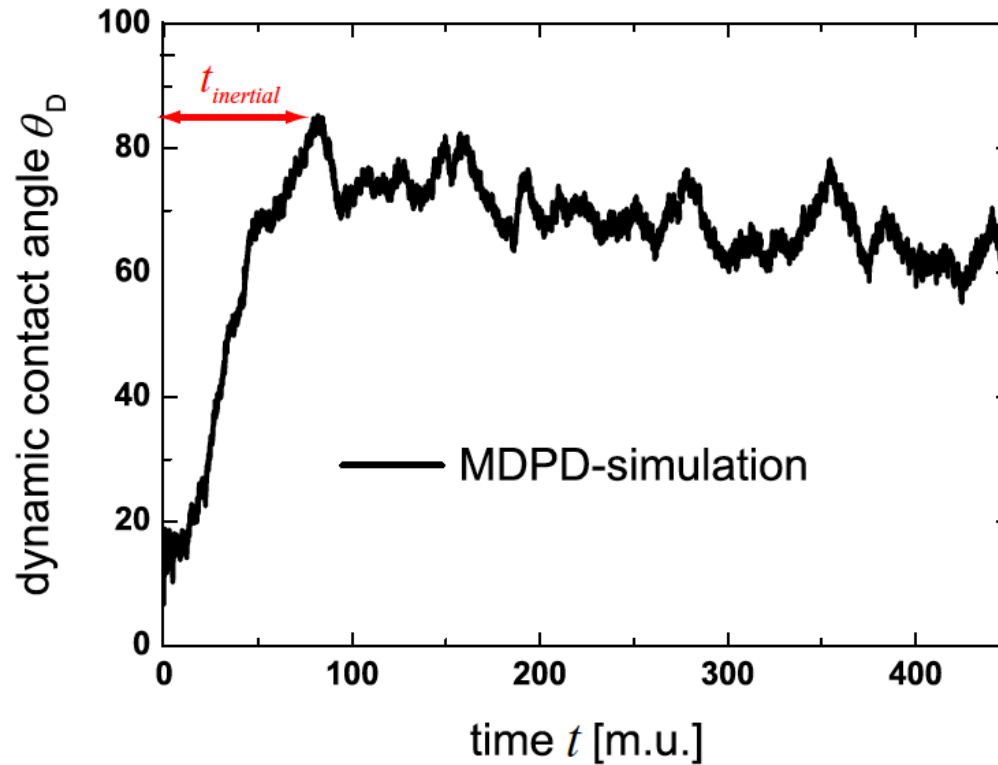
Figure 8. Dynamic contact angle behavior θ_d obtained by the MDPD-simulation versus time during the capillary filling process. Vertical axis in degrees.
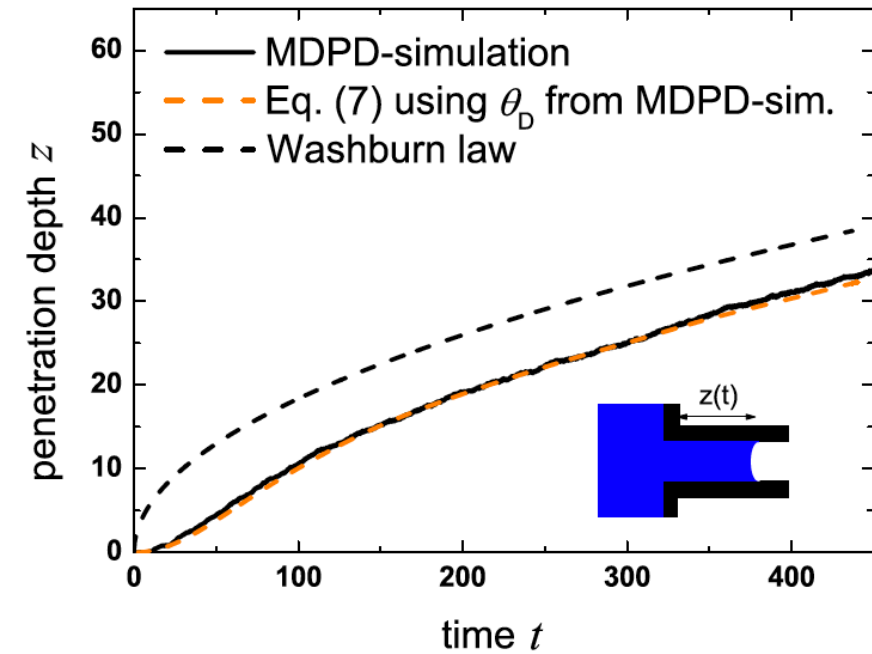
Figure 9. Dynamics of the penetration into the pore over time $z(t)$ obtained by the MDPD-simulation compared to equation (7). The dynamic contact angle is measured online during the simulation and inserted into equation (7) for the numerical integration.

DMC Examples

- **DMC reference:**
  - ☐ Theoretical foundations of dynamical Monte Carlo simulations by Fichthorn & Weinberg in J. Chem. Phys., 95, 1090 (1991).

Influence of Intermolecular Vibrations on the Electronic Coupling in Organic Semiconductors: The Case of Anthracene and Perfluoropentacene

Nicolas G. Martinelli,[a, b] Yoann Olivier,[a] Stavros Athanasopoulos,[a] Mari-Carmen Ruiz Delgado,[b] Kathryn R. Pigg,[b] Demétrio A. da Silva Filho,[b] Roel S. Sánchez-Carrera,[b] Elisabetta Venuti,[c] Raffaele G. Della Valle,[c] Jean-Luc Brédas,[a, b] David Beljonne,[a, b] and Jérôme Cornil*[a, b]
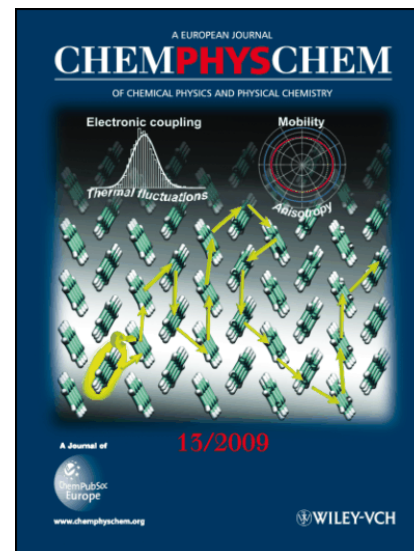
Martinelli et al.

- Objective: charge mobility in molecular crystals under lattice fluctuations

- Methods:
  - Crystal structure as the basis
  - MD simulation to sample intermolecular distances and orientations
  - Semiempirical method for transfer integrals
  - Marcus-Hush theory for charge hopping rates
  - DMC to obtain mobility…
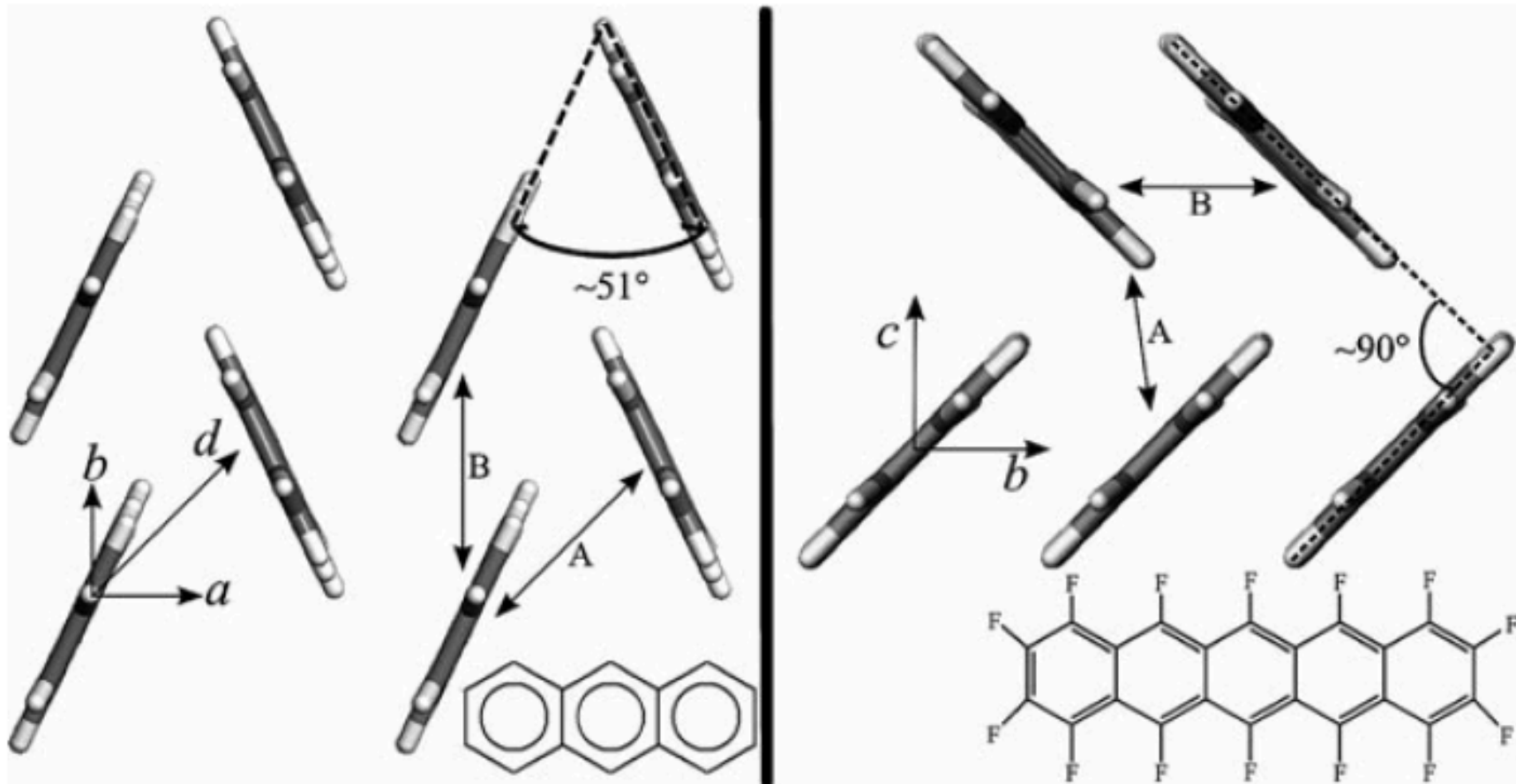
Figure 1. Representation of the crystal unit cell of anthracene (left) and fluorinated pentacene (right); the chemical structure of the two molecules and the labeling of the different dimers are also displayed.

Martinelli et al.
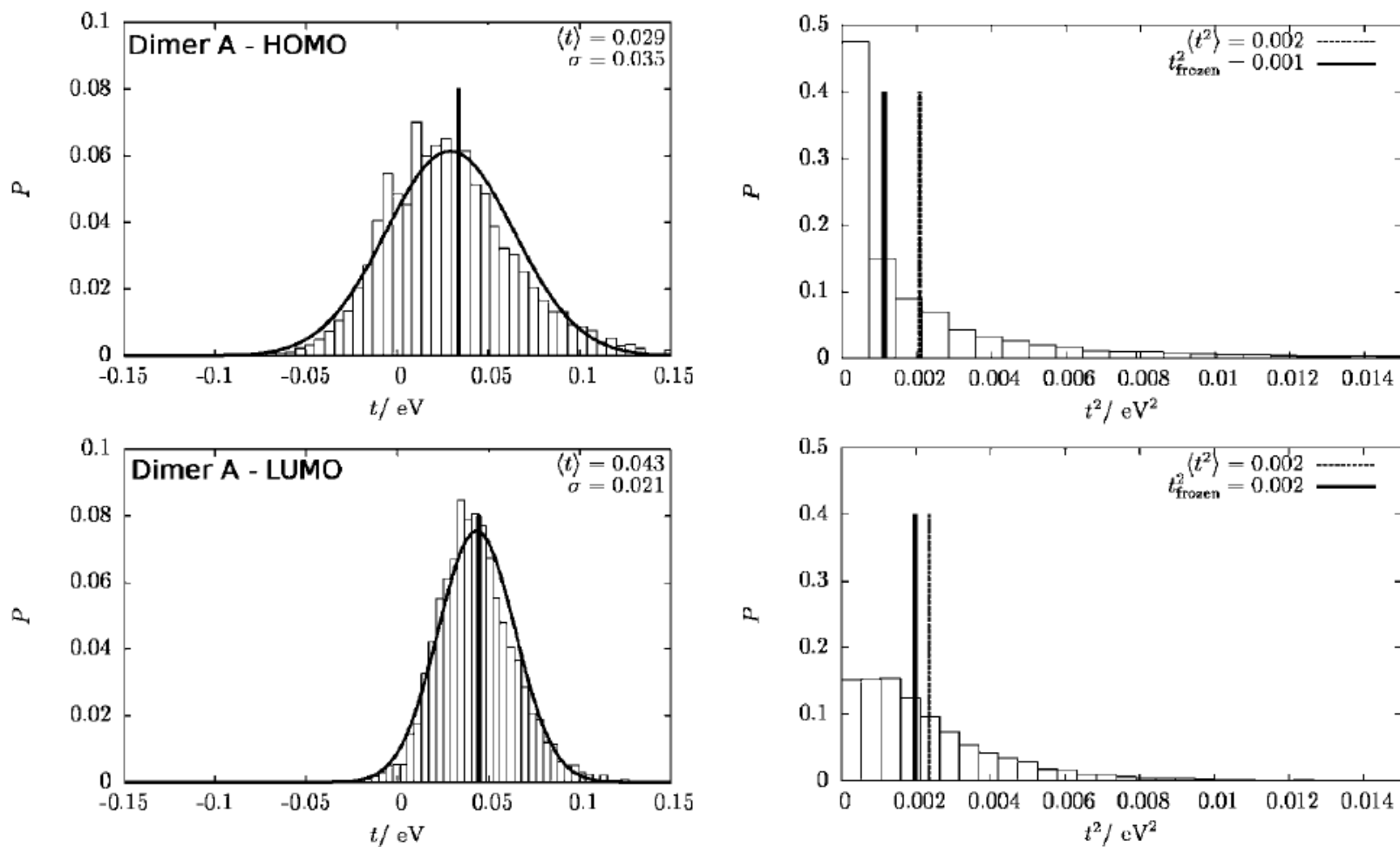
**Figure 2.** Probability distribution in arbitrary units of the transfer integrals for the HOMO (top) and LUMO (bottom) levels of dimer A in the anthracene unit cell, as extracted from 5000 snapshots generated with the COM-PASS force field. The transfer integrals calculated at the INDO level are reported both with their proper sign (left) and with their square value (right). When justified, the distribution has been fitted with a Gaussian function; the average value $\langle t \rangle$ and the standard deviation σ are also reported.
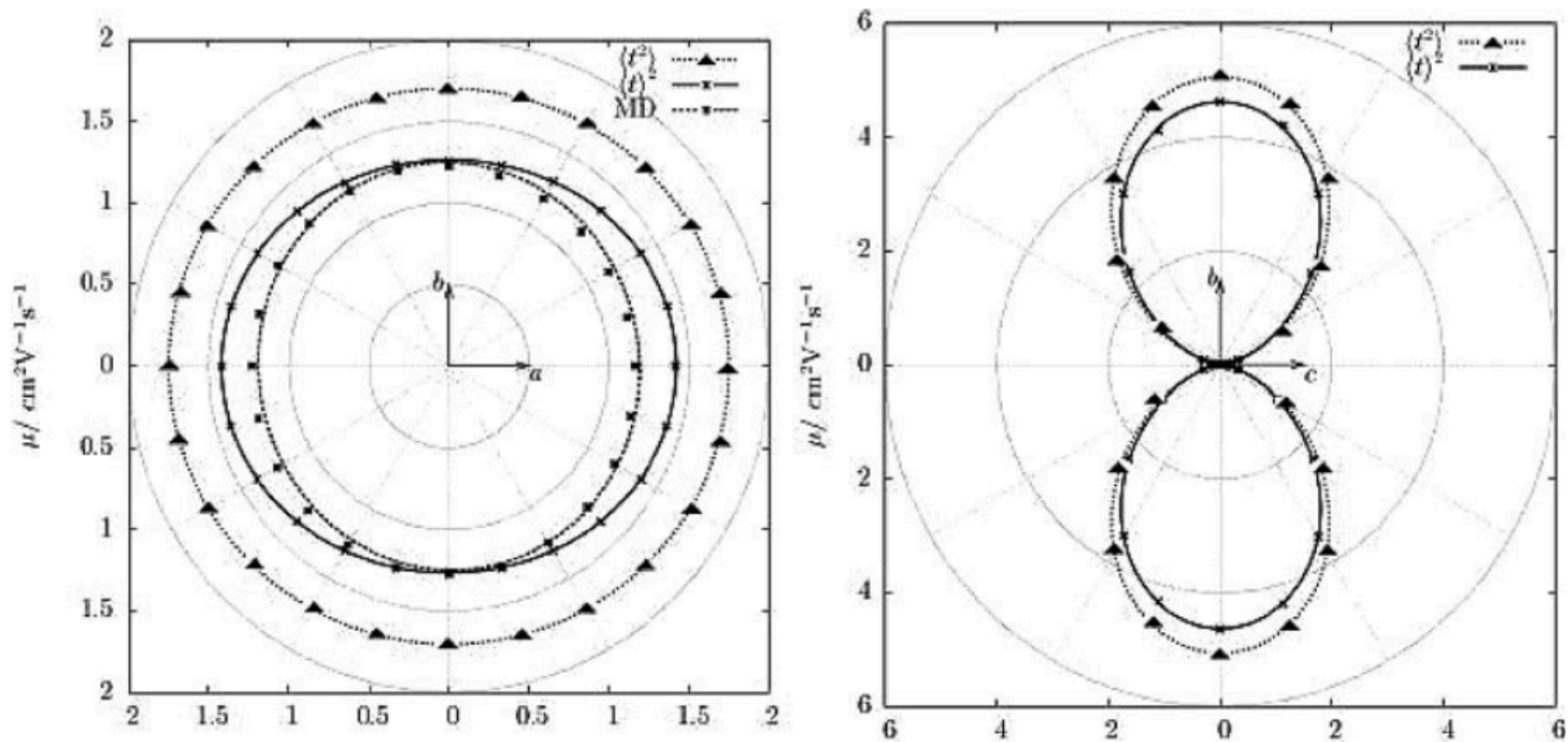
Figure 6. Polar plot of μ_e within the a–b plane for anthracene (left) and within the b-c plane for perfluoropenta-cene (right) crystal at $T=300$ K and for an applied electric field of 250 kV cm^{-1}. Triangles and dotted lines refer to MC simulations using the values of $\langle t^2 \rangle$ characteristic of the equilibrium structure (thermalized limit) and crosses with solid lines to MC simulations using the values of $\langle t \rangle^2$. In the left panel, bold crosses with dotted lines are associated to mobility values averaged over all MD snapshots within a static limit.
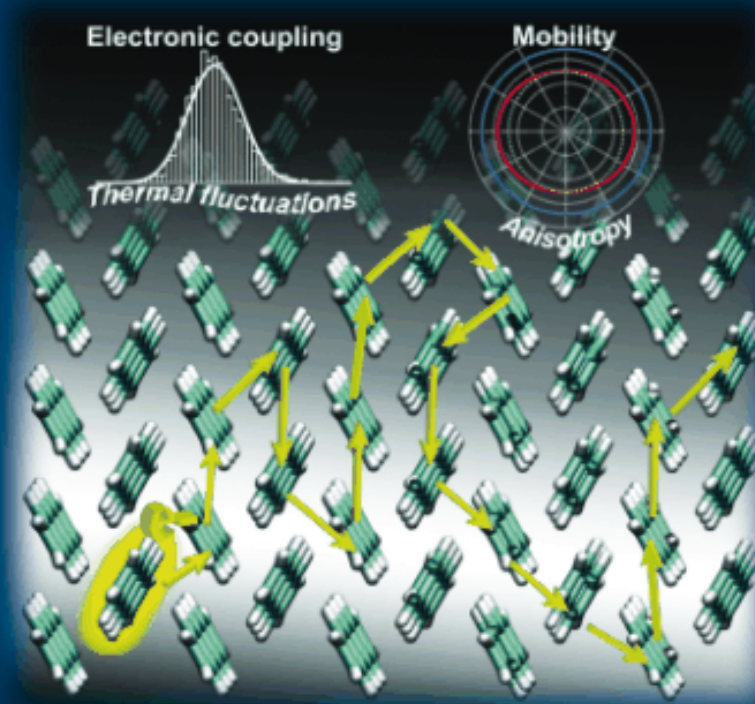
The role of collective motion in examples of coarsening and self-assembly†

Stephen Whitelam,‡[abc] Edward H. Feng,[b] Michael F. Hagan[d] and Phillip L. Geissler[bc]

The simplest prescription for building a patterned structure from its constituents is to add particles, one at a time, to an appropriate template. However, self-organizing molecular and colloidal systems in nature can evolve in much more hierarchical ways. Specifically, constituents (or clusters of constituents) may aggregate to form clusters (or clusters of clusters) that serve as building blocks for later stages of assembly. Here we evaluate the character and consequences of such collective motion in a set of prototypical assembly processes. We do so using computer simulations in which a system's capacity for hierarchical dynamics can be controlled systematically. By explicitly allowing or suppressing collective motion, we quantify its effects. We find that coarsening within a two dimensional attractive lattice gas (and an analogous off-lattice model in three dimensions) is naturally dominated by collective motion over a broad range of temperatures and densities. Under such circumstances, cluster mobility inhibits the development of uniform coexisting phases, especially when macroscopic segregation is strongly favored by thermodynamics. By contrast, the assembly of model viral capsids is not frustrated but is instead facilitated by collective moves, which promote the orderly binding of intermediates consisting of several monomers.
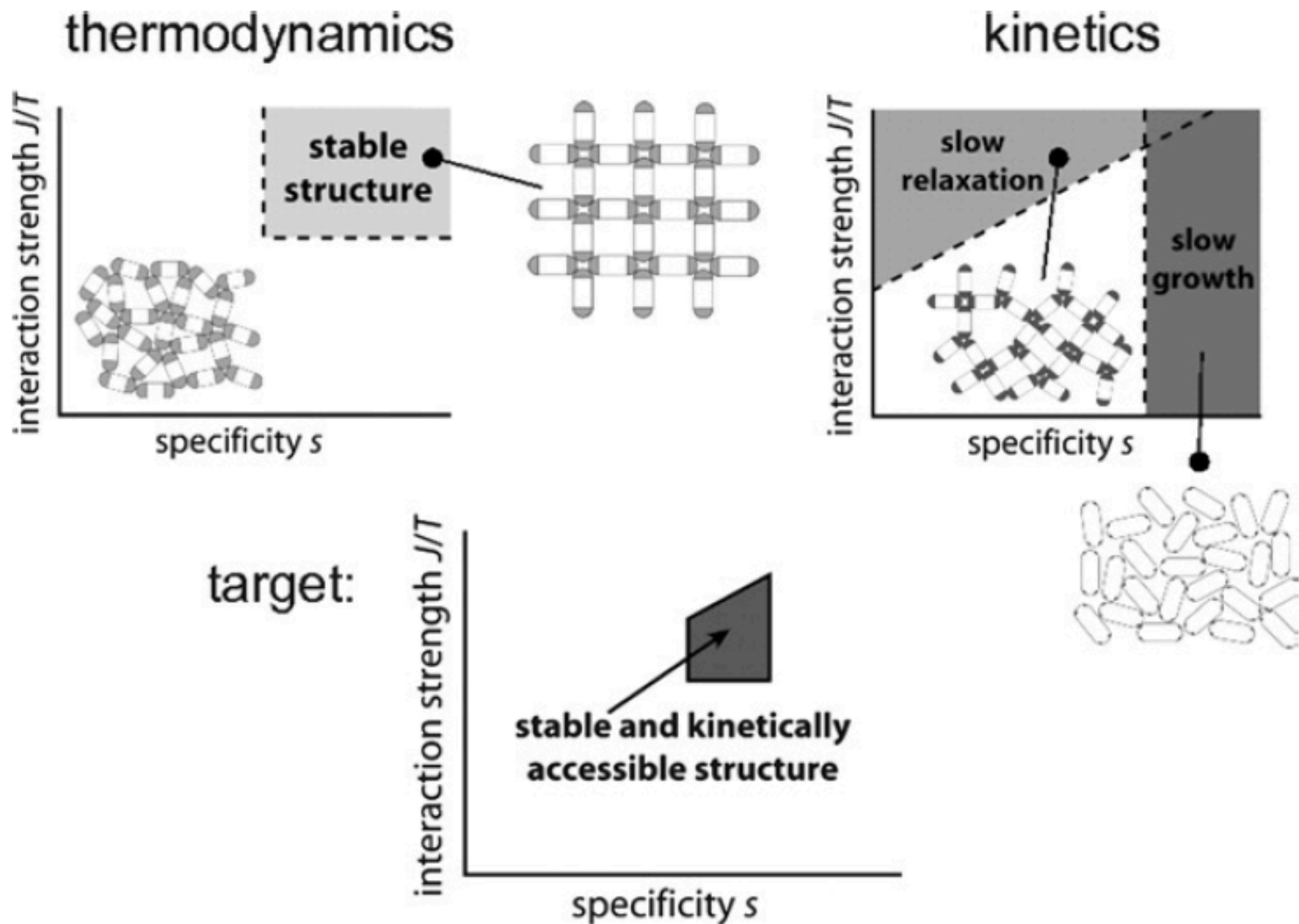
Fig. 1 The competitive nature of self-assembly: an illustration of the
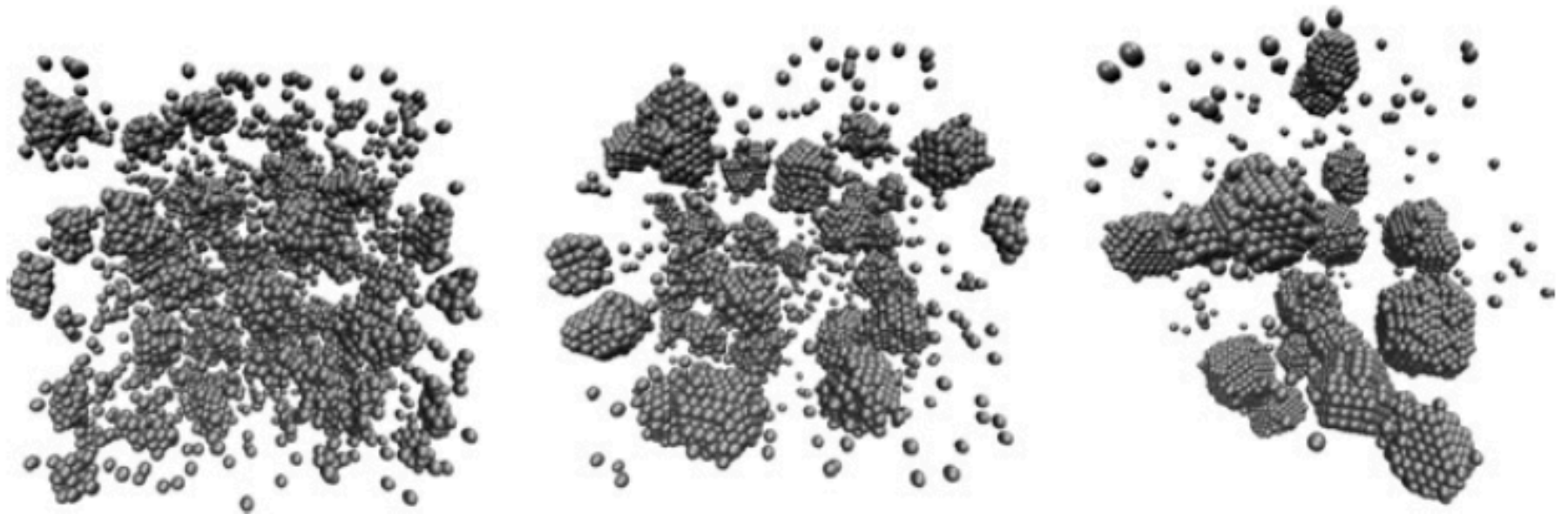
Fig. 11 Assembly pathway for system A under explicit collective moves. Assembly is driven principally by single-particle binding, unbinding and diffusion, with the effects of collective motion apparent only at late times when phase-separated clusters fuse. Times of image capture, in units of 10^6 MC steps, are from left to right 0.2, 0.6 and 1.4.
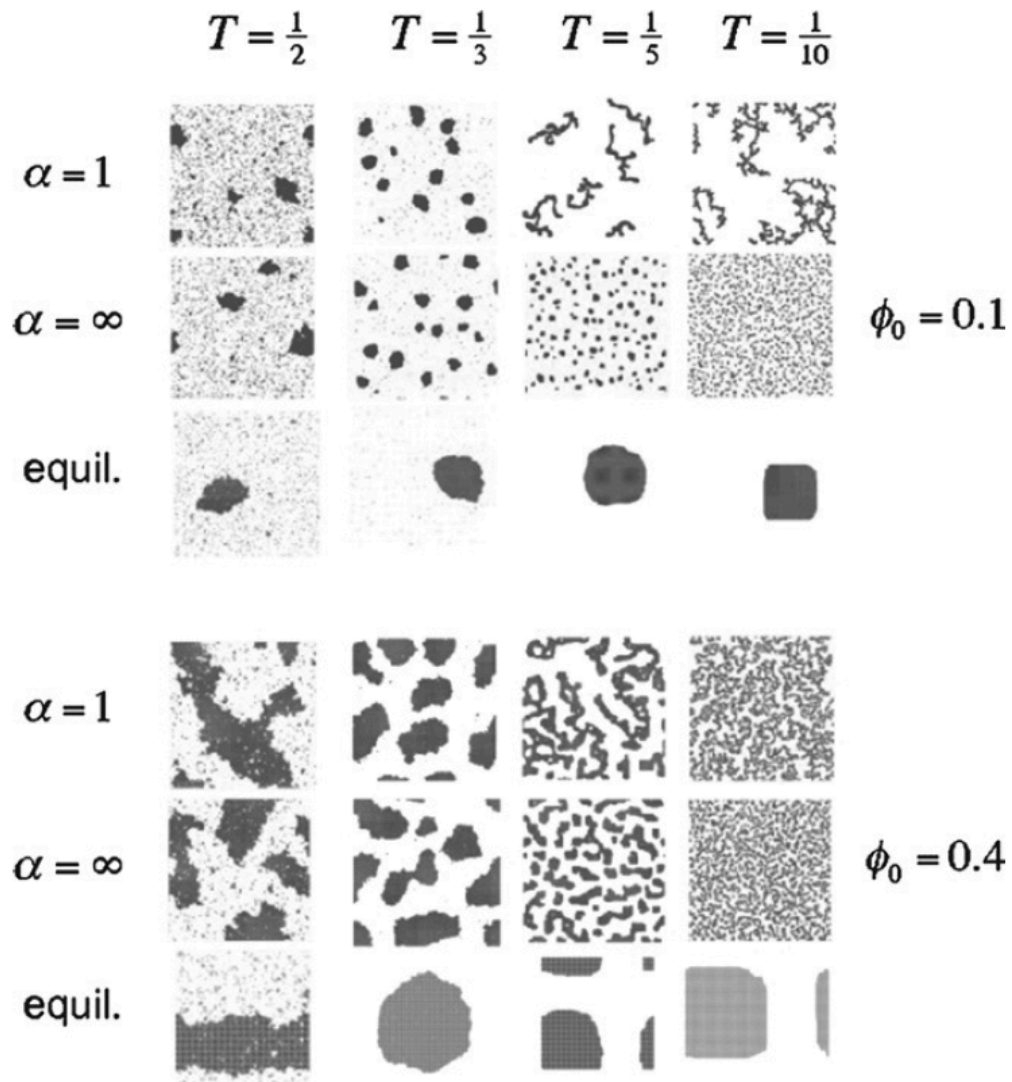
Fig. 6 Configurations of the lattice gas at fixed time following a quench from a disordered state, evolved using Monte Carlo dynamics with cluster diffusivity $D(n) \propto n^{-\alpha}$ and particle concentrations $\phi_0 = 0.1$ (top panel) and 0.4 (bottom panel). The equilibrium states (obtained using
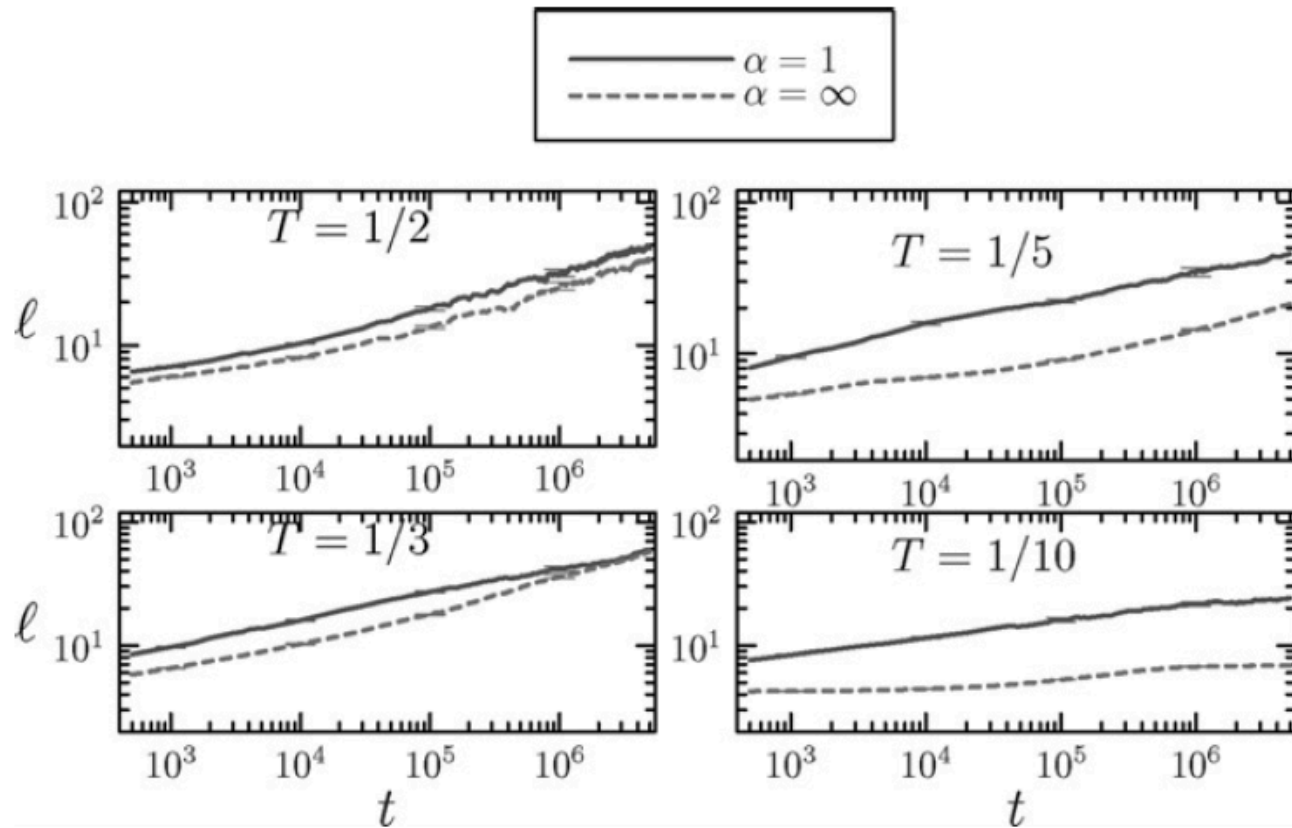
Fig. 7 Growth of domain size ℓ with Monte Carlo time t within the attractive lattice gas, for cluster diffusivity $\alpha = 1$ or $\alpha = \infty$ at particle concentration $\phi_0 = 0.1$ on a lattice of size $V = 256^2$. We perform quenches to $T = 1/2, 1/3, 1/5$ and $1/10$. Quantitative differences between dynamical protocols are seen even at the highest temperature. Data correspond to the mean of 10 trajectories; error bars are shown sparsely for clarity.
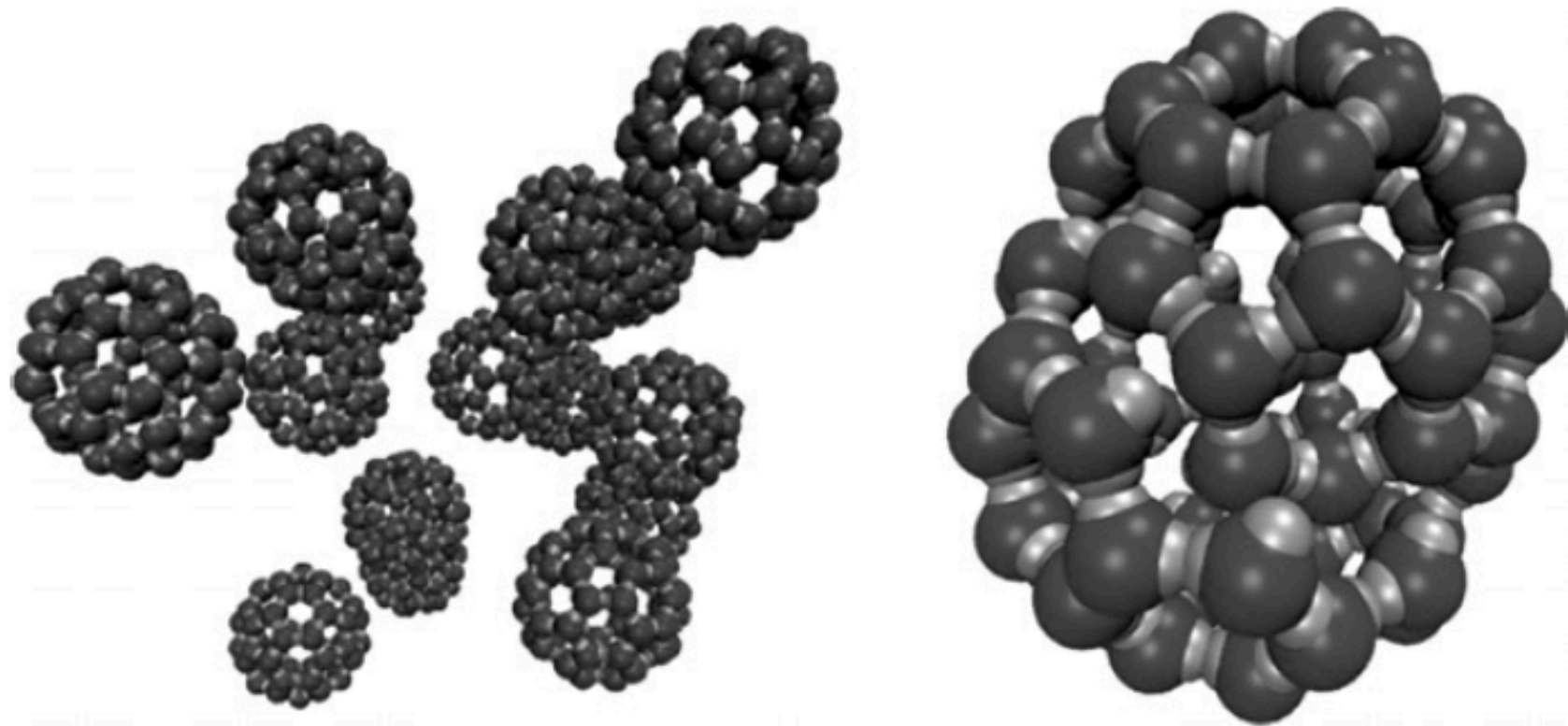
Fig. 13 Configurations of the capsid model generated using virtual-move Monte Carlo. Left: configuration illustrating high yield obtained at parameter set $\varepsilon_b = 16\,k_B T$, $\theta_m = 0.5$, $C_0 = 0.11$. Right: malformed shell of 76 particles obtained at parameter set $\varepsilon_b = 22\,k_B T$, $\theta_m = 0.5$, $C_0 = 0.037$.
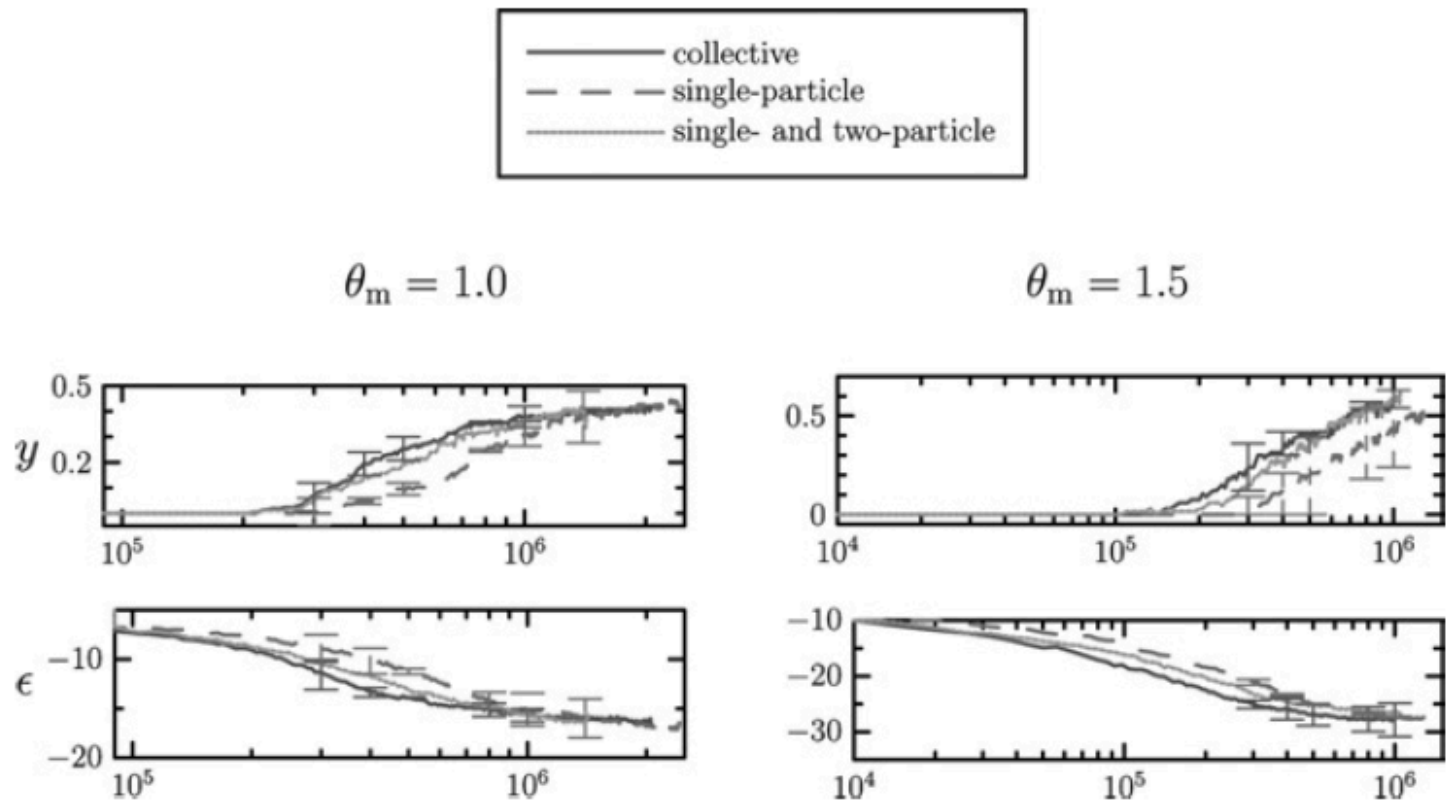
Fig. 14 Capsid kinetics at binding energy $\varepsilon_b = 14 k_B T$ and concentration $C_0 = 0.11$ evolved using Monte Carlo dynamics with different degrees of collective motion permitted. We show yield y and energy per particle ε as a function of time. Assembly under collective moves is more efficient than under single-particle moves. Restoring collective motion of dimers recovers a substantial fraction of the efficiency of fully collective motion. Data in the left panel are the mean of 10 trajectories, data in the right panel are the mean of 4 trajectories. Error bars are displayed sparsely for clarity.

Large-scale simulations of fluctuating biological membranes

Andrea Pasqua,[1,a)] Lutz Maibaum,[1,2,a),b)] George Oster,[3] Daniel A. Fletcher,[4,5] and Phillip L. Geissler[1,2,5]

[1]*Department of Chemistry, University of California, Berkeley, California 94720, USA*
[2]*Chemical Sciences Division, Lawrence Berkeley National Laboratory, Berkeley, California 94720, USA*
[3]*Department of Molecular and Cellular Biology, University of California, Berkeley, California 94720, USA*
[4]*Department of Bioengineering, University of California, Berkeley, California 94720, USA*
[5]*Physical Biosciences Division, Lawrence Berkeley National Laboratory, Berkeley, California 94720, USA*

We present a simple, and physically motivated, coarse-grained model of a lipid bilayer, suited for micron scale computer simulations. Each ≈ 25 nm^2 patch of bilayer is represented by a spherical particle. Mimicking forces of hydrophobic association, multiparticle interactions suppress the exposure of each sphere's equator to its implicit solvent surroundings. The requirement of high equatorial density stabilizes two-dimensional structures without necessitating crystalline order, allowing us to match both the elasticity and fluidity of natural lipid membranes. We illustrate the model's versatility and realism by characterizing a membrane's response to a prodding nanorod. © 2010 American Institute of Physics. [doi:10.1063/1.3382349]
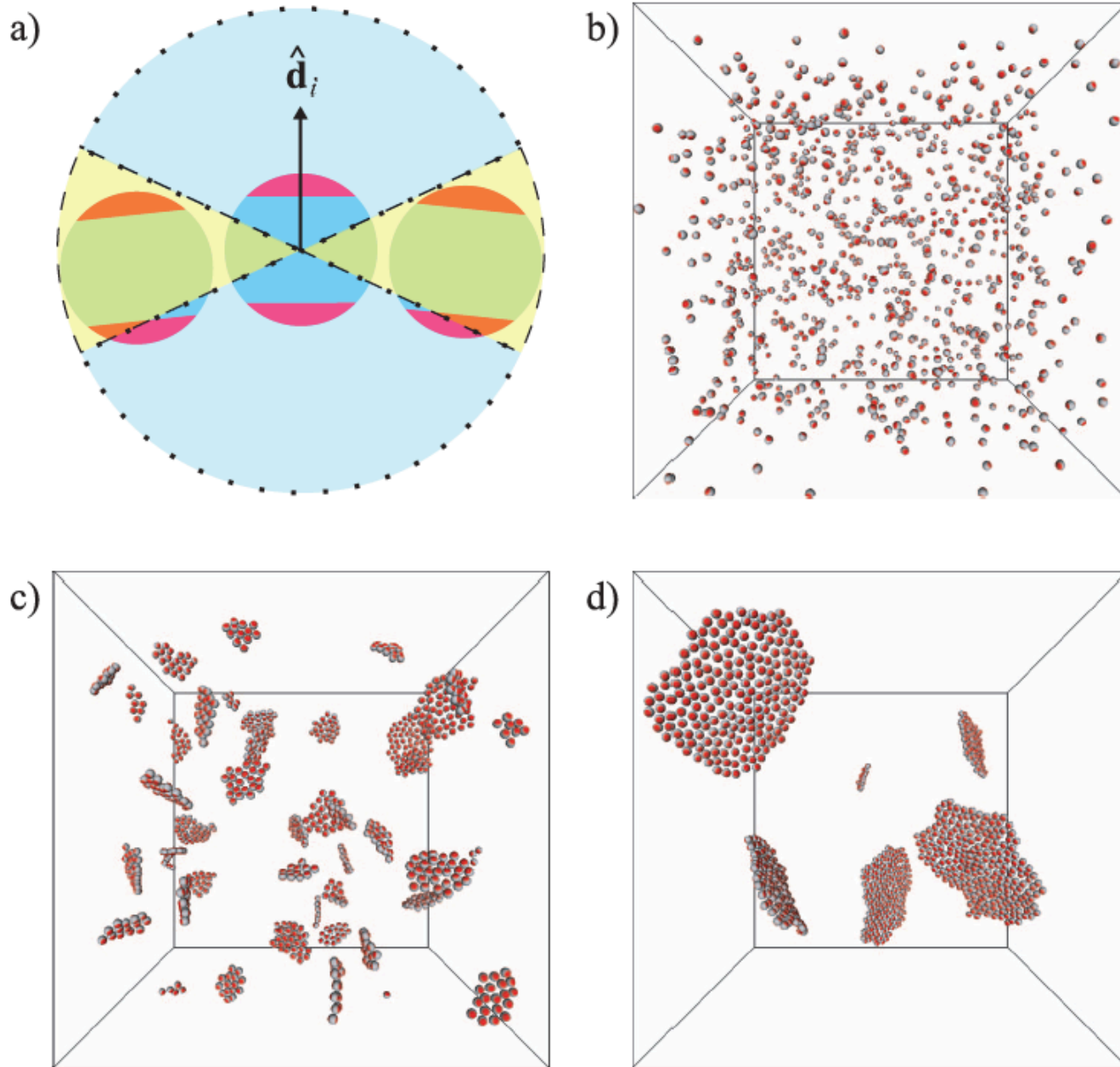
FIG. 1. (a) Illustration of our model. Each particle corresponds to a fragment of lipid bilayer, comprised of a central hydrophobic core and two surrounding hydrophilic layers. The unit vector $\hat{\mathbf{d}}_i$ specifies the orientation of particle i. Also shown are the spatial regions used to compute the numbers of equatorial (enclosed by dashed line) and polar (enclosed by dotted line) neighbors of particle i. (b) Random initial configuration for a trajectory of $N=864$ particles. As time progresses, particles quickly form two-dimensional patches that continue to coarsen. Shown are snapshots after (c) 100 and (d) 1000 Monte Carlo sweeps.
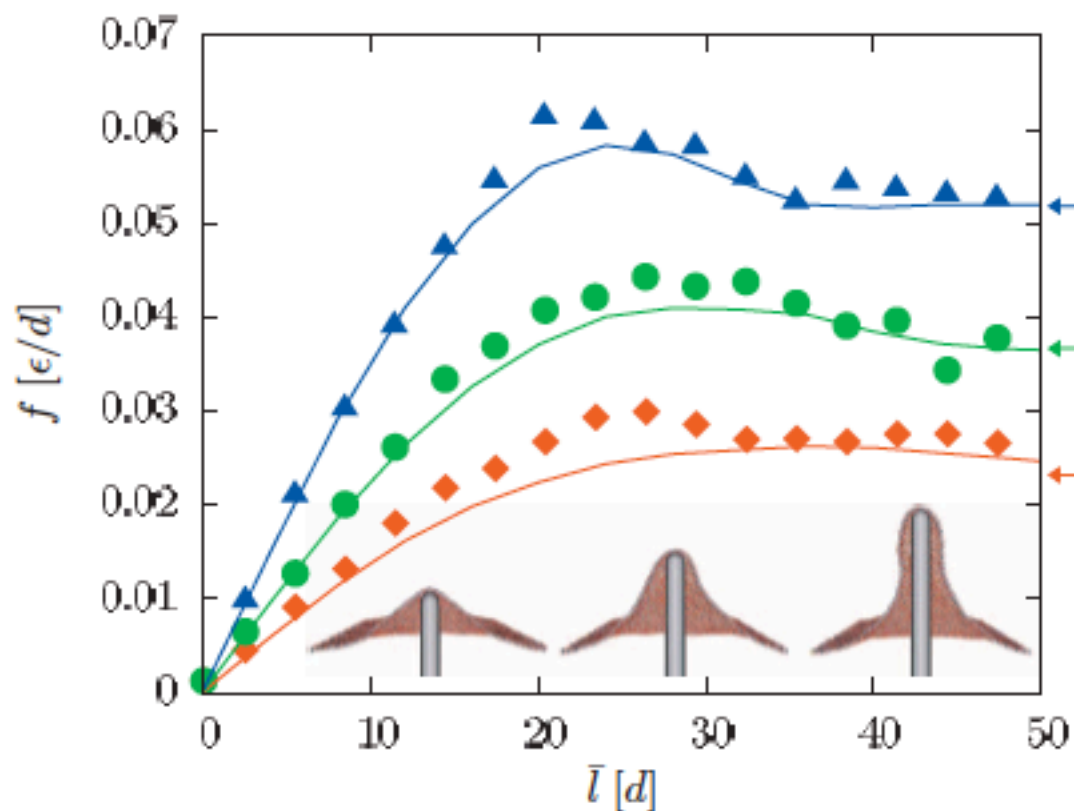
FIG. 3. Restoring force as a function of protrusion length for three different values of the lateral tension τ: $0.0002\epsilon/d^2$ (squares), $0.0005\epsilon/d^2$ (circles), and $0.001\epsilon/d^2$ (triangles). For each value of τ and l_0 we performed computer simulations at two values of K (0.2 and 1 in units of ϵ/d^2). The force
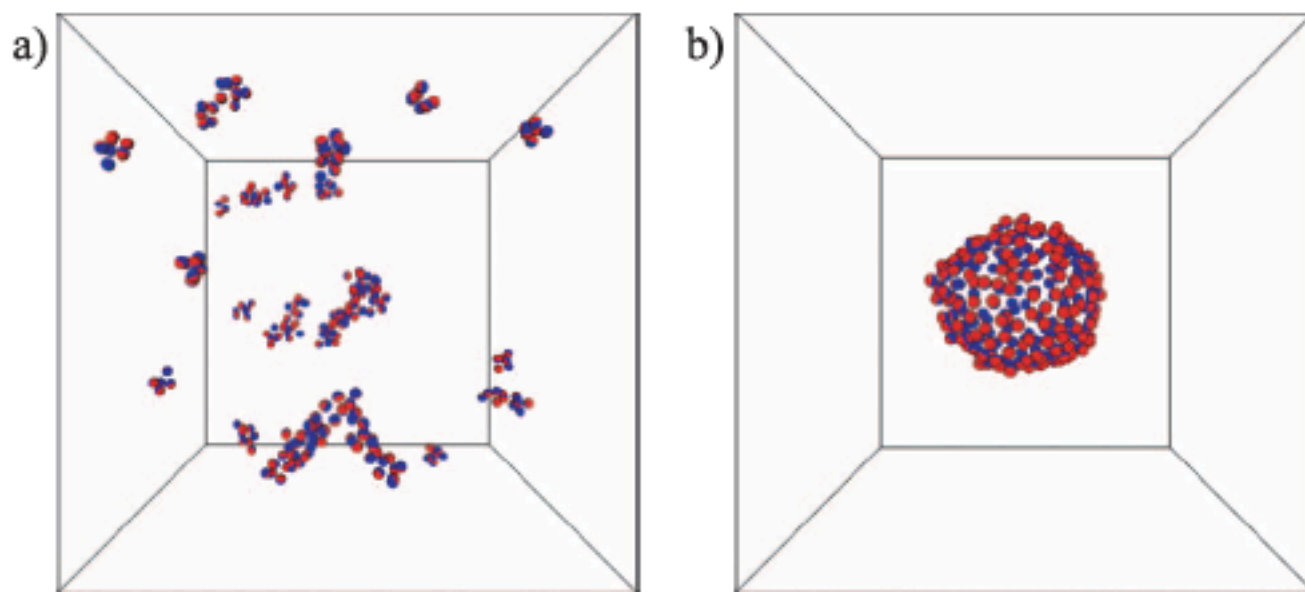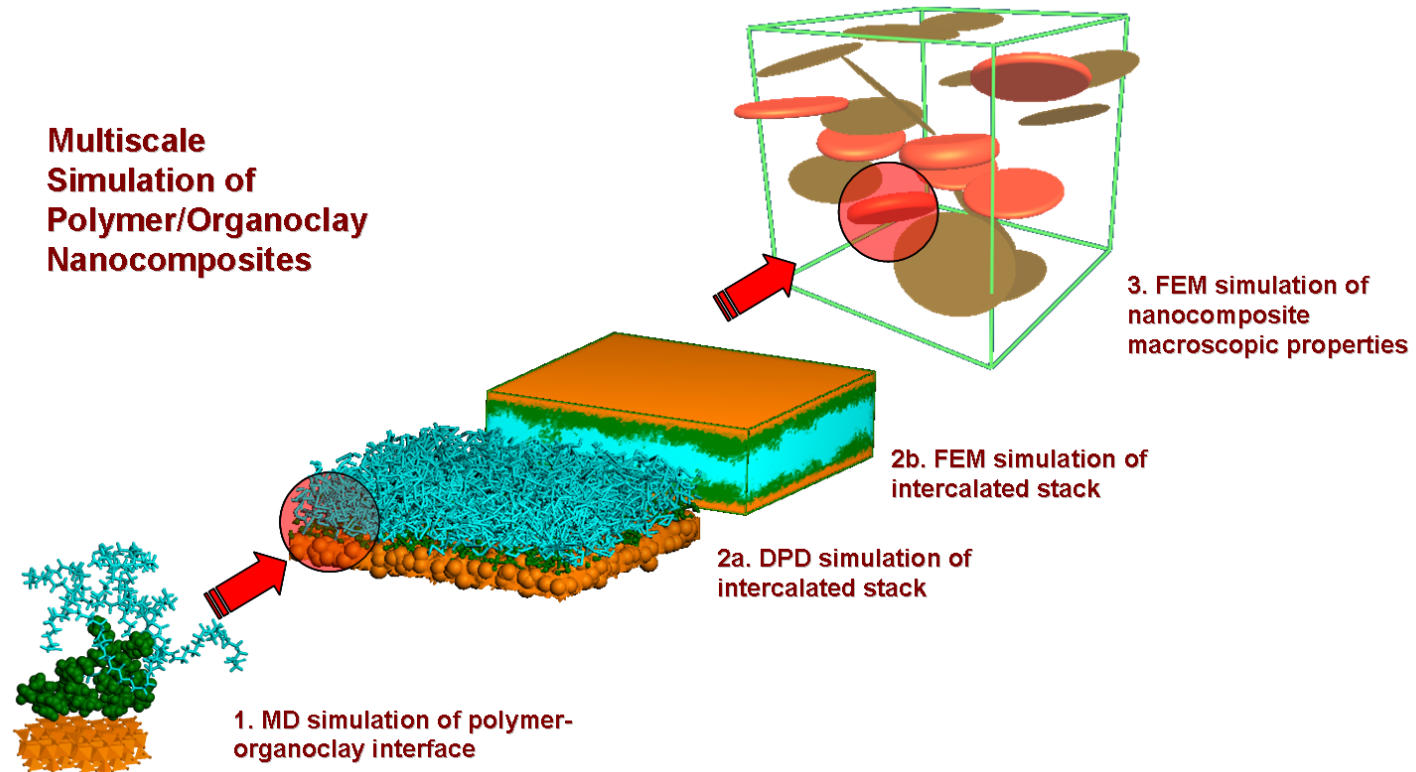
FIG. 4. (a) Typical configuration of the membrane model developed by Drouffe and co-workers ($\alpha = \eta = 1$, $T = 1.6\epsilon$). A flat sheet of 256 particles with parallel orientation vectors was used as the initial configuration. This structure dissolves quickly into a disordered collection of small clusters. (b) Final configuration of a trajectory starting from the same initial state, but employing an alternative parameter set ($\alpha = 1$, $\eta = -1$, and $T = 0.5\epsilon$). The initially flat sheet remains stable, and closes to form a vesicle.

Multiscale Modeling

Multiscale Simulation of Polymer/Organoclay Nanocomposites

1. MD simulation of polymer-organoclay interface

2a. DPD simulation of intercalated stack

2b. FEM simulation of intercalated stack

3. FEM simulation of nanocomposite macroscopic properties

http://m3.dti.supsi.ch/index.php/research/multiscale-simulation/

Remarks

- Multiscale CG methods useful for modeling bulk properties & dynamics

- Multiscale view: QM → MM → MD/MC → BD/DPD/DMC → FEM…

- A map of molecular modeling methods, hopefully enough for understanding literatures and initializing future research…